Oxygen Vacancies induced electron traps in Tungsten doped Bi_2MoO_6

for Enhanced Photocatalytic Performance

Chang Sun,[ab] Zitong Zhao,[ab] Hougang Fan,[*abc] Yanli Chen,[abc] Xiaoyan Liu,[abc] Jian Cao,[abc] Jihui Lang,[abc] Maobin Wei,[abc] Huilian Liu[abc]   Lili Yang[*abc]
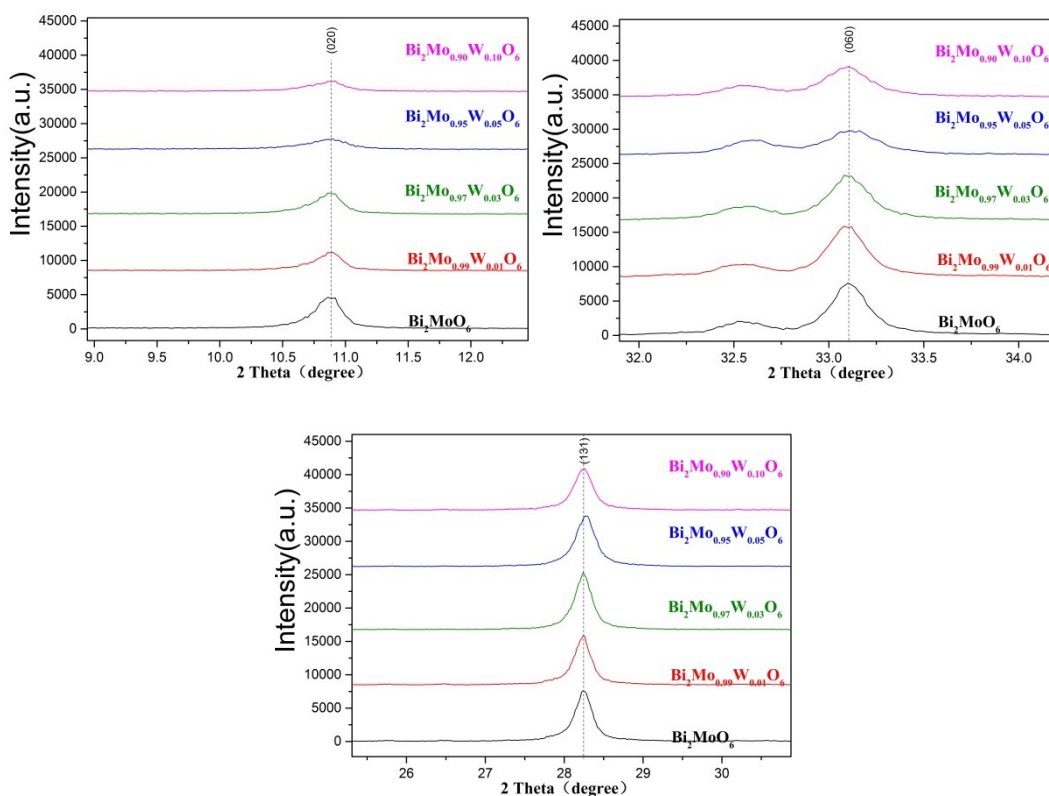
Fig. S1 The enlarged XRD patterns of (131), (060) and (020) peaks for the $Bi_2Mo_{1-x}W_xO_6$ samples

Table S1. The lattice constant of the $Bi_2Mo_{1-x}W_xO_6$ samples.

	a(Å)	b(Å)	c(Å)	Vol (Å³)
Bi_2MoO_6	5.499	16.215	5.491	489.61
$Bi_2Mo_{0.99}W_{0.01}O_6$	5.500	16.218	5.492	489.91
$Bi_2Mo_{0.97}W_{0.03}O_6$	5.501	16.222	5.488	489.71
$Bi_2Mo_{0.95}W_{0.05}O_6$	5.499	16.217	5.490	489.56
$Bi_2Mo_{0.90}W_{0.10}O_6$	5.500	16.222	5.490	489.89

Table S2 The grain size (nm) of the $Bi_2Mo_{1-x}W_xO_6$ samples.

	x=0.00	x=0.01	x=0.03	x=0.05	x=0.10
Grain size	29.0±1.7	29.2±1.9	27.5±2.2	20.6±4.8	24.2±3.2
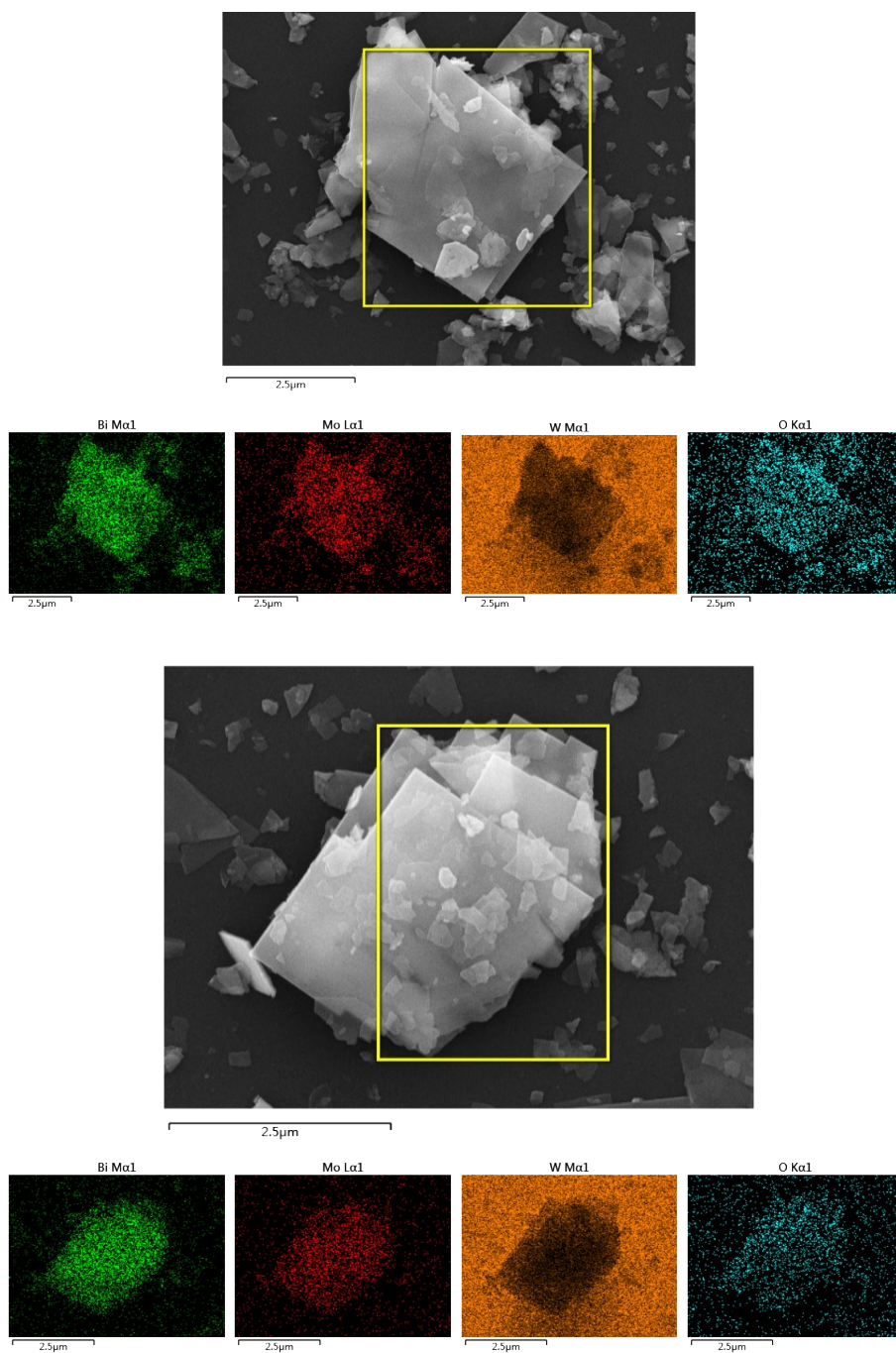
Fig. S2 Element mapping of $Bi_2Mo_{0.95}W_{0.05}O_6$ sample
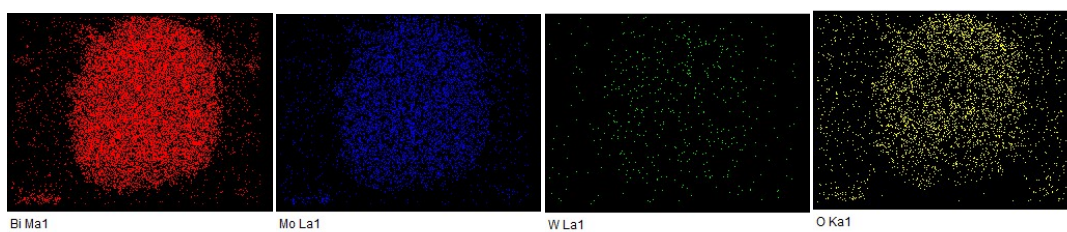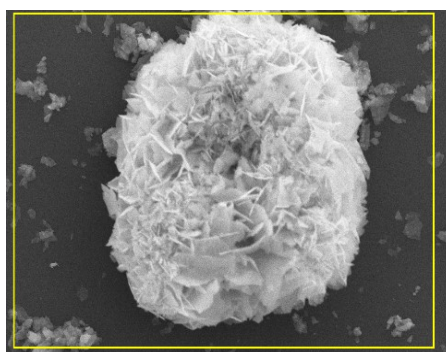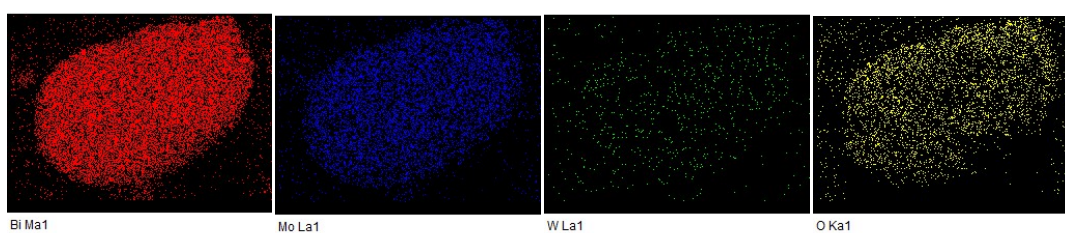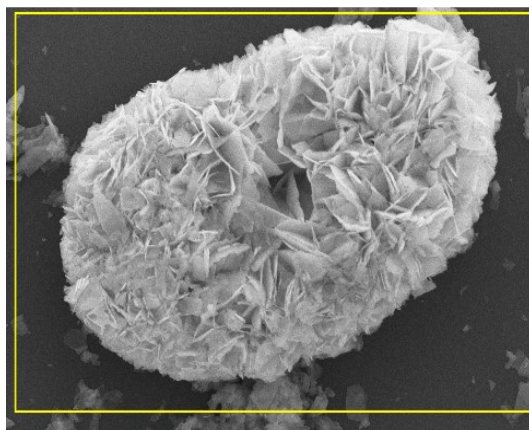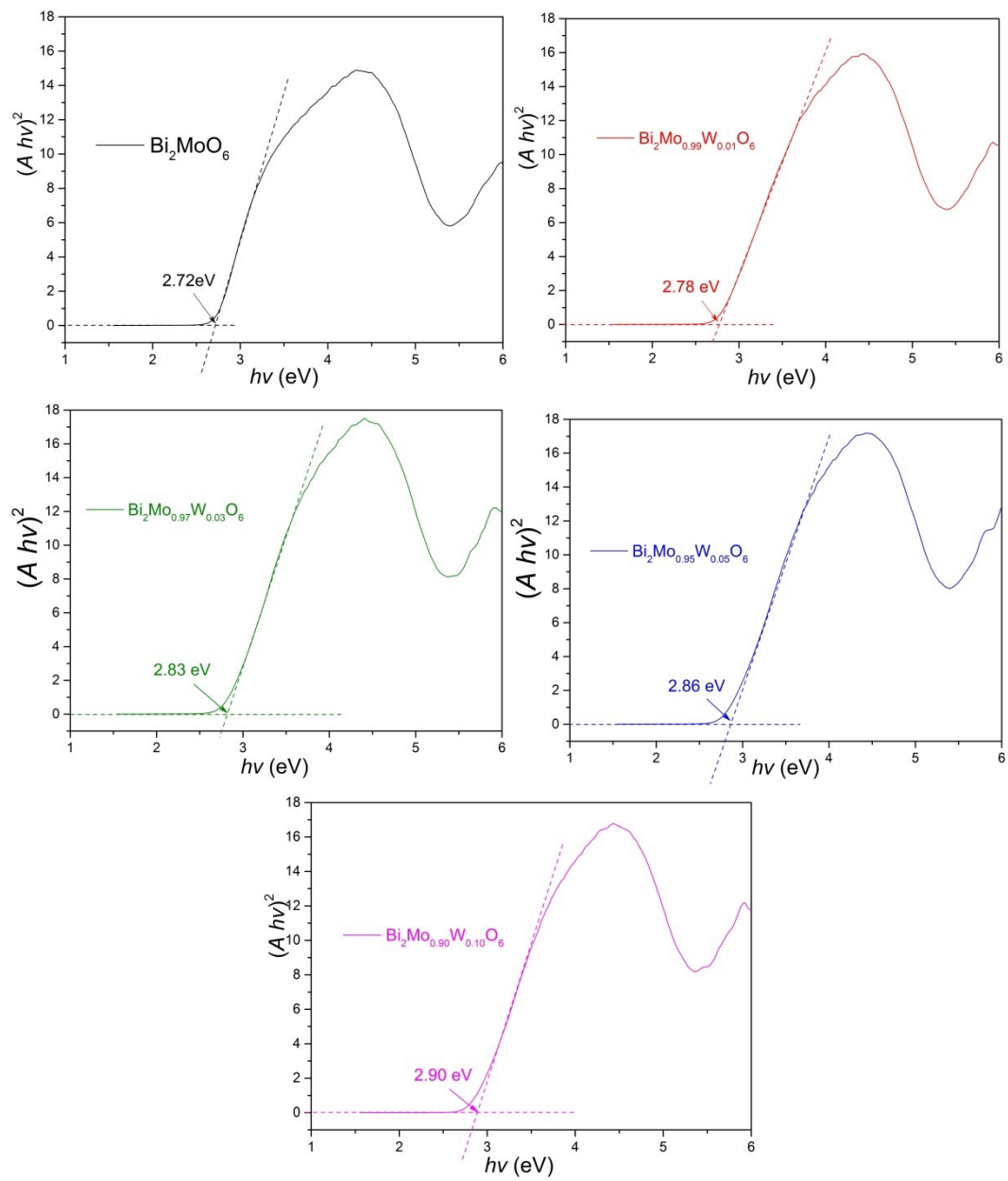
Fig S3. Element Mapping of $Bi_2Mo_{0.90}W_{0.10}O_6$ sample

Fig. S4 The band gap of $Bi_2Mo_{(1-x)}W_xO_6$ samples through Tauc plot.
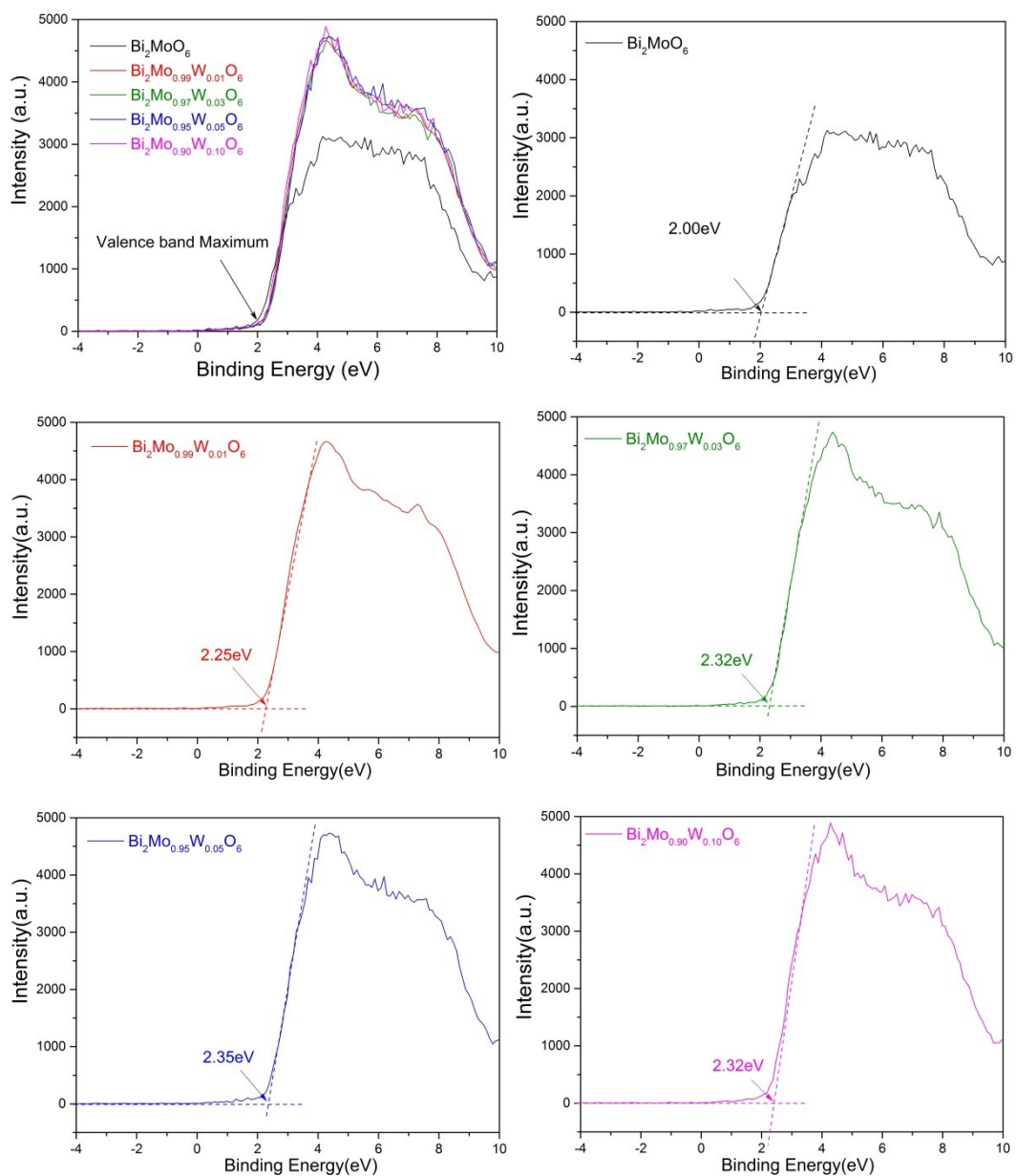
Fig. S5 The valence band maximum of $Bi_2Mo_{(1-x)}W_xO_6$ samples.
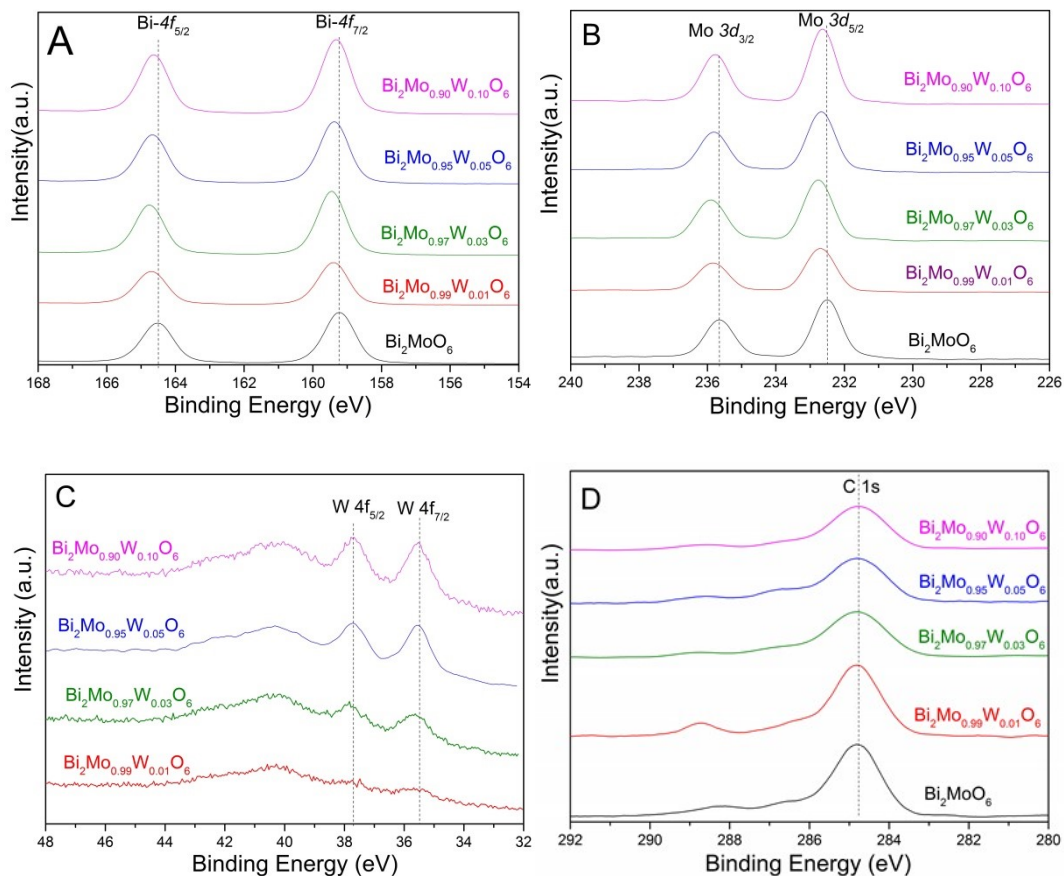
Fig. S6 The high resolution XPS scans over (A)Bi 4f, (B)Mo 3d, (C)W 4f and (D)C 1s peaks of $Bi_2Mo_{1-x}W_xO_6$ samples.

Table S3 The atomic percentages of every element in the $Bi_2Mo_{(1-x)}W_xO_6$ samples

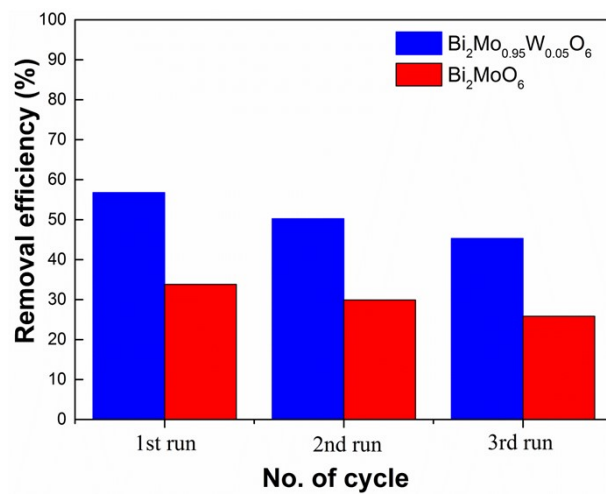| Atomic %	Bi 4f	Mo 3d	W 4f	O 1s
Bi_2MoO_6	18.95	9.93	/	71.12
$Bi_2Mo_{0.99}W_{0.01}O_6$	20.29	9.71	0.14	69.85
$Bi_2Mo_{0.97}W_{0.03}O_6$	22.13	10.05	0.31	67.51
$Bi_2Mo_{0.95}W_{0.05}O_6$	21.07	9.41	0.52	69.00
$Bi_2Mo_{0.90}W_{0.10}O_6$	21.59	9.66	0.54	68.21

Fig. S7 The reusability of the Bi_2MoO_6 and $Bi_2Mo_{0.95}W_{0.05}O_6$ samples for RhB removal.